Electronic Supplementary Material (ESI) for Journal of Materials Chemistry A.
This journal is © The Royal Society of Chemistry 2024

Supporting Information

Enhancing healability and degradability of epoxy via synergetic steric and electron-withdrawing effects for green electrical packaging

Lei Zhang, Wenjie Sun, Zhongqi Guo, Tianyu Li, Yi Zhou, Chenglong Wu, Yonghong Cheng*

State Key Laboratory of Electrical Insulation and Power Equipment, School of Electrical Engineering, Xi'an Jiaotong University, Xi'an 710049, PR China
E-mail: lzhangac@xjtu.edu.cn

Supplementary Methods

1. Insulating properties experiments

AC/DC breakdown strength were evaluated on a computer-controlled breakdown instrument (GJW-100kV, Changchun, China) with a plate-plate electrode system. The electrodes and the samples with a thickness of ca. 0.2 mm were immersed in silicone oil to avoid surface flashover. The applied voltage was increased with a rate of 2 $kV \cdot s^{-1}$ until the sample got a breakdown. The breakdown strength was evaluated by the Weibull analysis according to Equation (S1).

$$P(E) = 1 - \exp\left[-\left(\frac{E}{E_0}\right)^{\beta}\right] \quad \text{(S1)}$$

whereby P is the failure probability, E is the measured electrical breakdown strength, E_0 is the scale parameter, and the β is the shape parameter. In total, ten samples for each type of material were tested for Weibull analysis.

2. Reprocessing performance experiments

The samples were ground into powder, followed by hot-pressing under 20 MPa at different temperatures for 30 min. Reprocessability (γ) was quantified based on mechanical and insulating performance by calculating the property recovery ratio of the recycled specimens ($P_{\text{reprocessed}}$) to the original specimen (P_{original}).

$$\gamma = \frac{P_{\text{reprocessed}}}{P_{\text{original}}} \times 100\% \tag{S2}$$

where P is tensile strength for mechanical reprocessability, and breakdown strength for electrical reprocessability.

3. Mechanical healability experiments

The rectangular film was cut into two parts by a clean blade, and then the separated sample pieces were closely placed, followed by heating at 180 ℃/3 MPa for different time. The change in the sample morphology was observed through a polarizing microscope (BX51–P). The healing efficiency (η) was calculated as the ratio of the tensile strength of the healed specimen (P_{healed}) to the original specimen (P_{original}).

$$\eta = \frac{P_{\text{healed}}}{P_{\text{original}}} \times 100\% \tag{S3}$$

4.Electrical treeing healability experiments

A needle-plate electrode configuration was used for electrical treeing initiation and propagation, whereby the steel needle electrode with a tip radius of 25±5 μm is embedded in the sample. The sample size is 30×15×3 mm^3. The insulation distance between the needle tip and the plate electrode is 2.0 mm. The prepared samples were immersed in silicone oil to avoid surface discharges, and AC voltage (15 kV/50 Hz) was applied to the samples for 15 min at room

temperature. The morphologies of electrical trees in epoxy were recorded. The damaged samples were healed at 180 ℃/15 MPa for 30 min.

The characteristic length (l) and the duty ratio (D) of electrical tree were used to describe the morphology of electrical treea. The characteristic length of electrical trees refers to the length of the electrical treea in the direction of the electric field. The duty ratio of electrical trees is mainly used to describe the size of the electrical trees area within a selected region of solid material. A fixed-size region (50×50 pixels) covering the growth range of electrical trees is selected from the electrical tree images. Subsequently, the number of black pixels in this region is counted and divided by the total number of pixels in the region, yielding the duty ratio of the electrical tree.

5. Degradation and recyclability experiments

The cured epoxies underwent immersion in a dibutyl amine at 180 ℃. The degradation rate (v_d) is calculated as the following equation：

$$v_d = \frac{(m_0 - m_r)}{t_d \cdot V} \times 100\% \quad \text{(S4)}$$

where m_0 is the original weight of the sample, m_r is the mass of the degraded sample after deionized water washing and drying, t_d is the degradation time and V is the applied volume of dibutyl amine. The morphologies of glass fiber before and after degradation were obtained using a scanning electron microscope (SEM, GEMINI 500, ZEISS). Besides, the morphologies and the major element of high voltage resistor before packaging, packaged and after degradation of EP-HUB-DFXD were analyzed by EDS-mapping (Phenom ProX)

6. Computer simulation of urea bonds parameters

The grounds state carbamids (S_0) and corresponding two dissociated fragments (D_0) were all optimized by density functional theory (DFT) with B3LYP functionals and the 6-31G* basis

set through Gaussian 09W. The bond energy was calculated according to the differences between the two D_0 radical fragments and the S_0 carbamids, i.e.,

$$E_{\text{bond}} = E_{\text{frag1}} + E_{\text{frag2}} - E_{\text{carbamid}} \quad \text{(S5)}$$

The main hindered urea bond unit in various epoxy samples were selected to conduct the computer simulation, including the HUB-DA, HUB-BA and HUB-FA. Table S2 presents the optimized structure.

Supplementary Figures and Tables

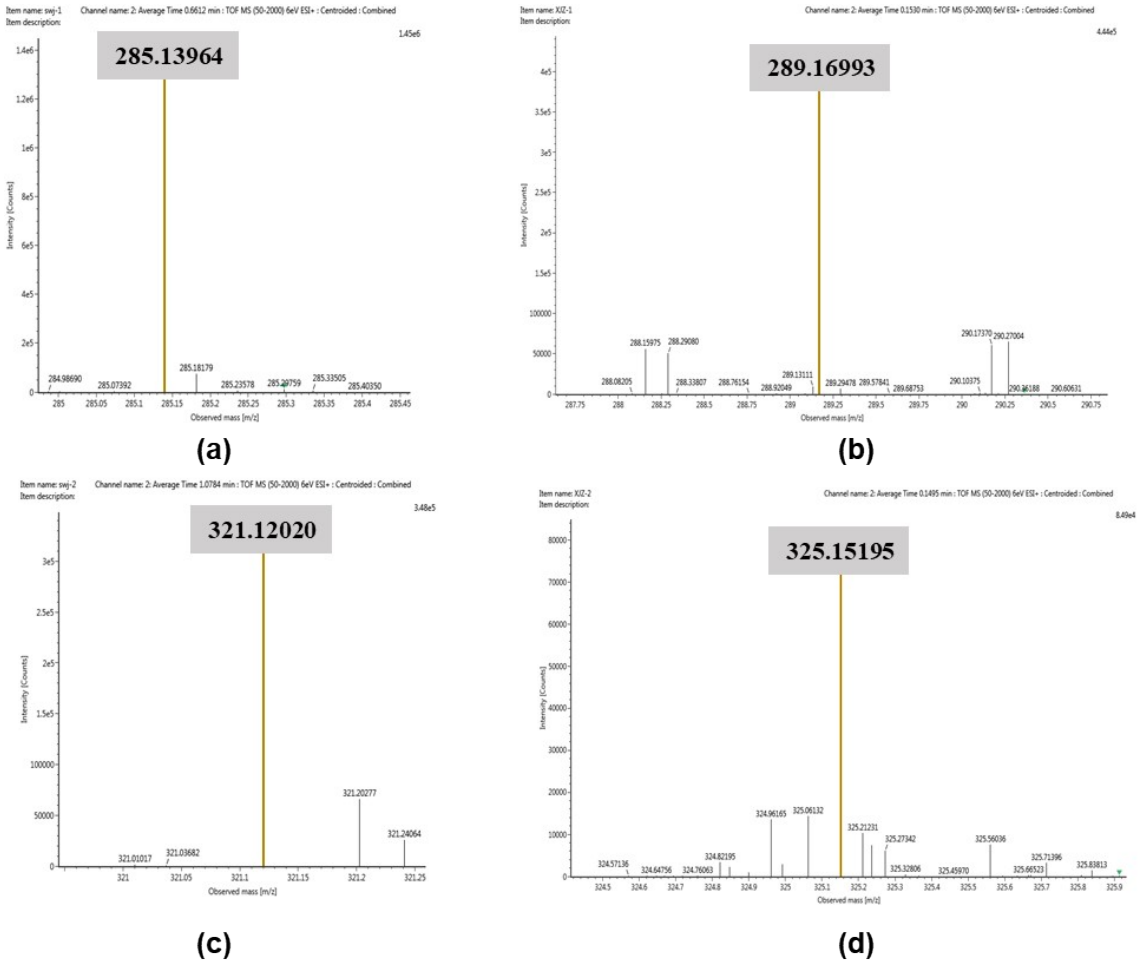

Figure S1. (a) Mass spectrum of DXDim measured with an Ultra Performance Liquid Chromatography-Quadrupole-Time of Flight Mass Spectrometer (UPLC-Q-TOF-MS, WATERS I Class VION IMS, 1 mg/mL in acetonitrile). The calculated theoretical molecular mass of DXD is 284.13, where the detected m/z is 285.13964 (corresponding to the M+1 peak, the same below). (b) Mass spectrum of DXD. The calculated theoretical molecular mass of DXD is 288.16, where the detected m/z is 289.16993. (c) Mass spectrum of DFXDim. The calculated theoretical molecular mass of DFXD is 320.34, where the detected m/z is 321.12020. (d) Mass spectrum of DFXD. The calculated theoretical molecular mass of DFXD is 324.14, where the detected m/z is 325.15195.

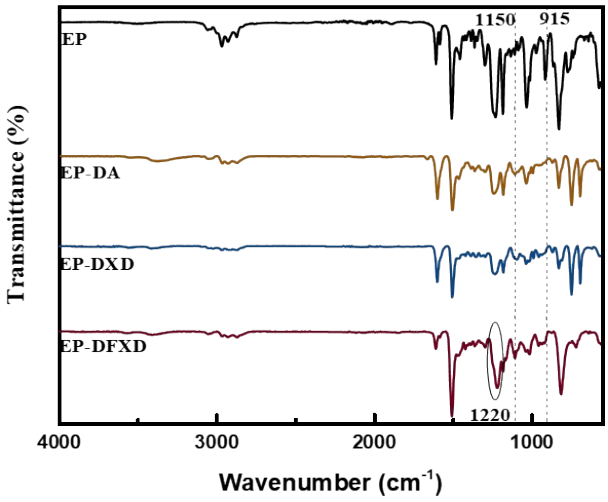

Figure S2. FTIR curves of amine-terminated epoxy.

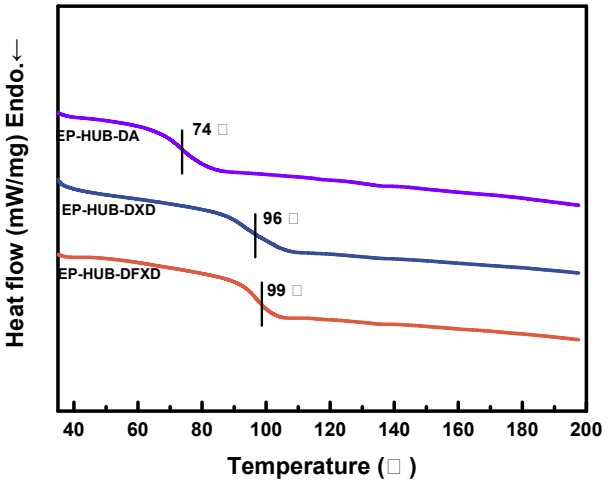

Figure S3. DSC curves of the prepared epoxy.

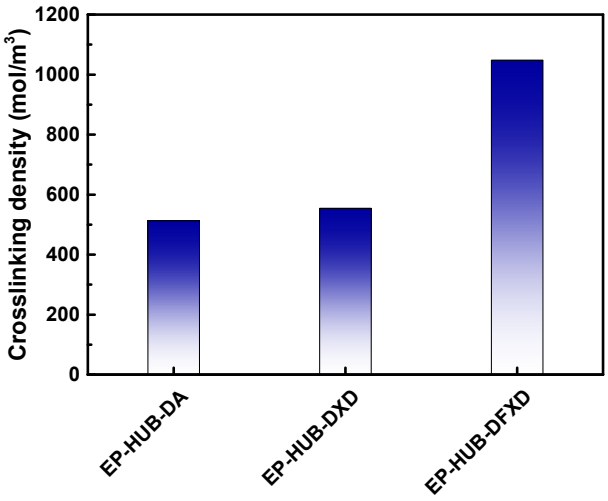

Figure S4. Crosslinking density of the prepared epoxy.

Table S1. Mechanical properties of the prepared epoxy

Samples	σ^a (MPa)	ε^b (%)	E^c(MPa)
EP-HUB-DA	40.6±1.62	7.9±0.22	572±7.9
EP-HUB-DXD	41.8±1.63	7.0±0.40	626±35.3
EP-HUB-DFXD	43.1±2.85	6.5±0.55	699±39.3

[a]Tensile strength; [b]Elongation at break; [c]Elastic modulus.

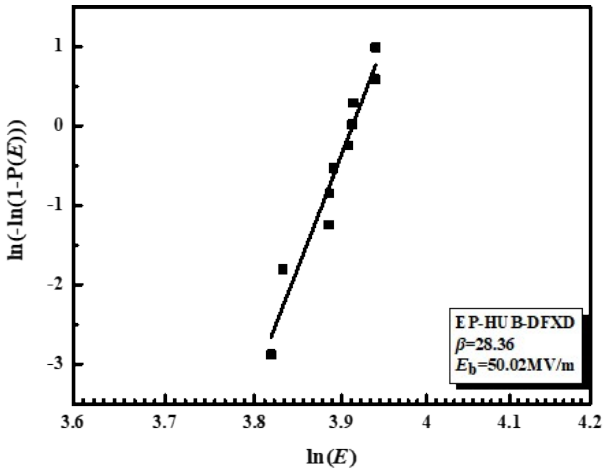

Figure S5. Weibull plots of the breakdown strength of EP-HUB-DFXD with a thickness of 1 mm.

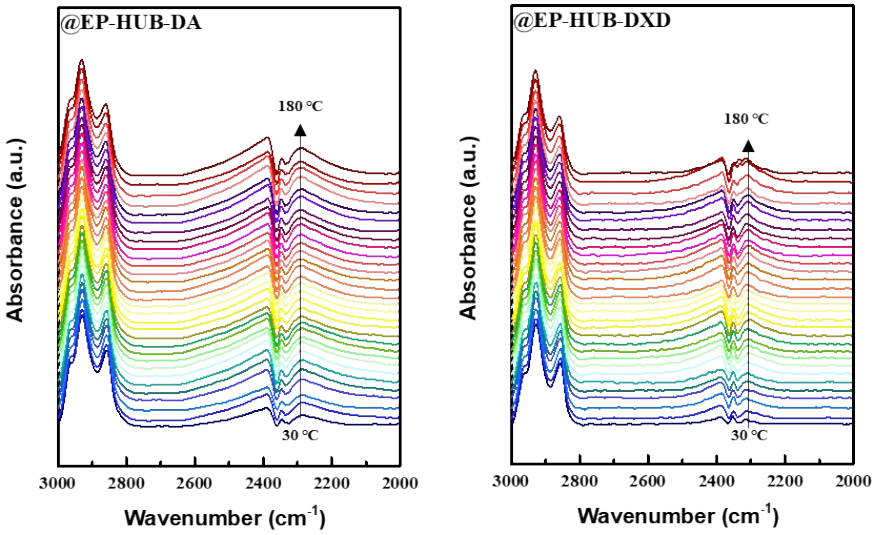

Figure S6. Temperature-dependent FTIR spectra of the EP-HUB-DA and EP-HUB-DXD.

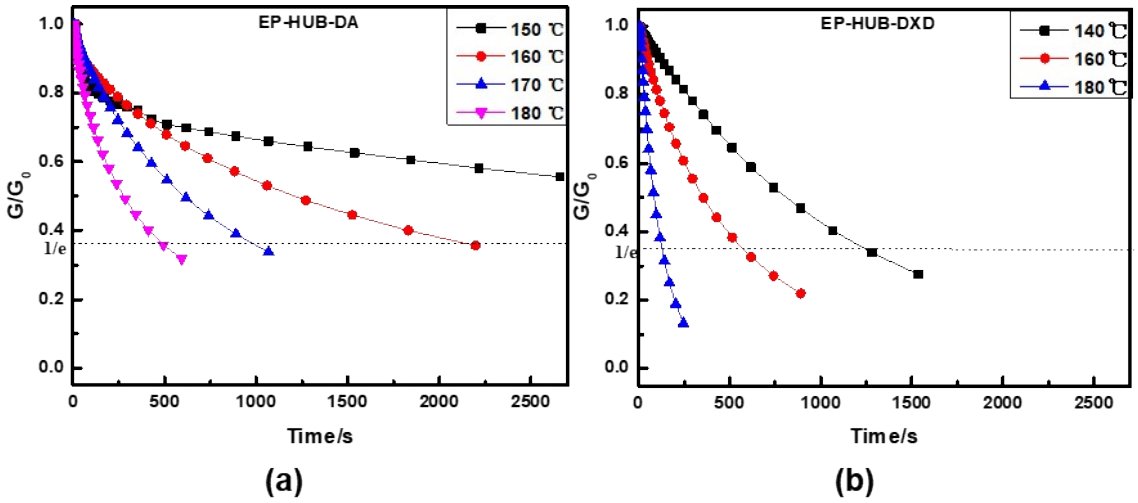

Figure S7. Normalized stress relaxation curves of EP-HUB-DA and EP-HUB-DXD.

Table S2. The optimized structure of hindered urea bonds with different molecular structure after chemical calculation

Molecular structure	Optimized structure		
	S_0	D_0-1	D_0-2
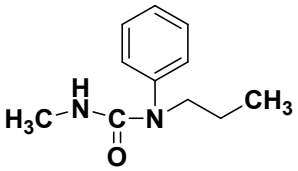 HUB-DA	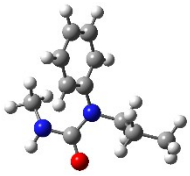	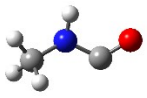	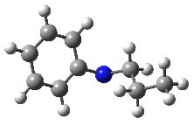
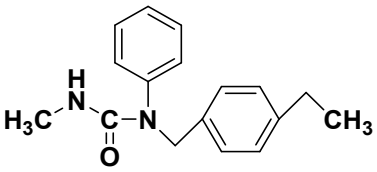 HUB-DXD	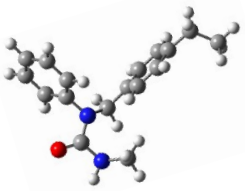	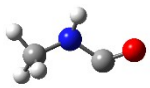	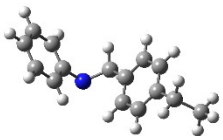
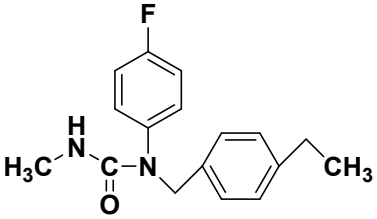 HUB-DFXD	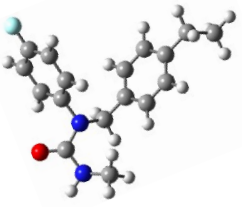	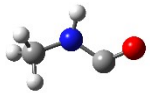	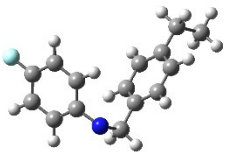

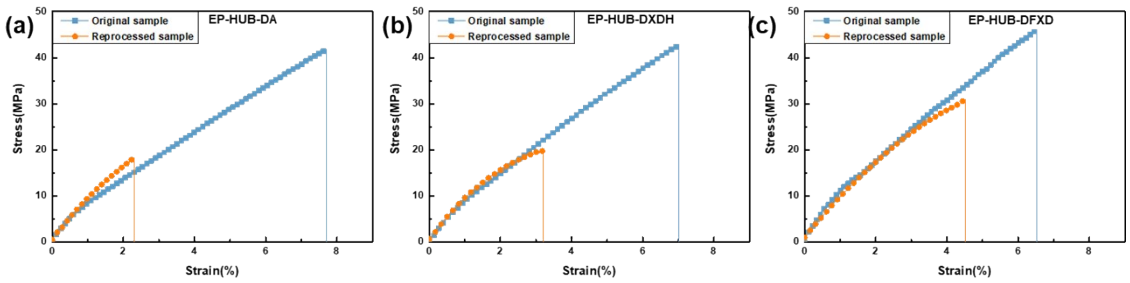

Figure S8. Stress–strain curves of epoxy containing hindered urea bonds with different molecular structures before and after reprocessing.

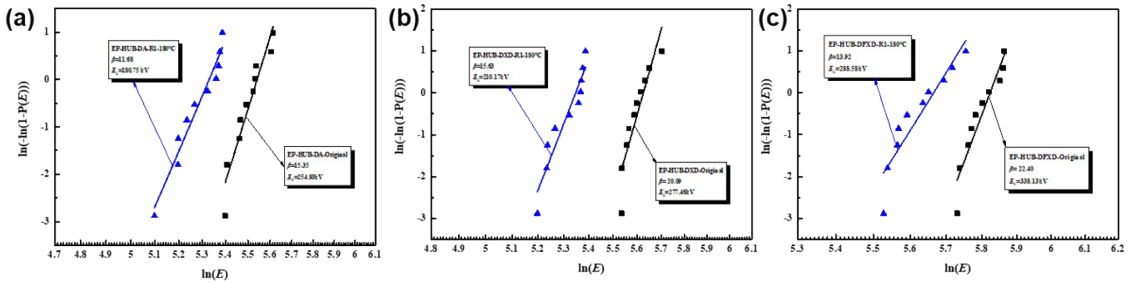

Figure S9. Weibull plots of the DC breakdown strength of epoxy containing hindered urea bonds with different molecular structures before and after reprocessing.

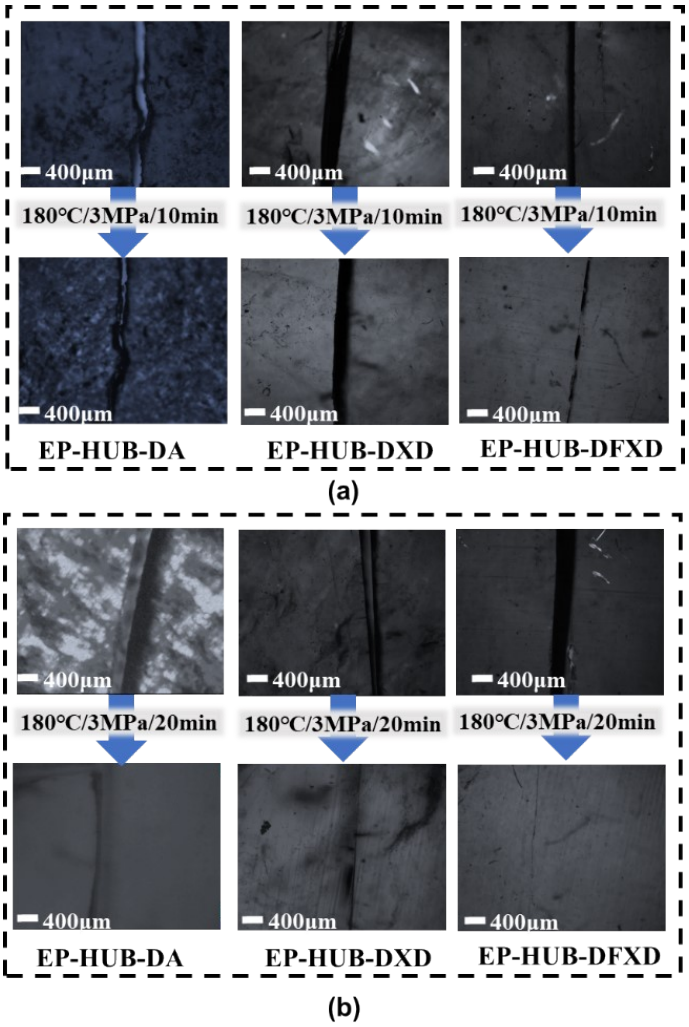

Figure S10. Micrographs of cut samples before and after healing. (a) The healing condition is 180 °C/3 MPa/10 min, (b) The healing condition is 180 °C/3 MPa/20 min.

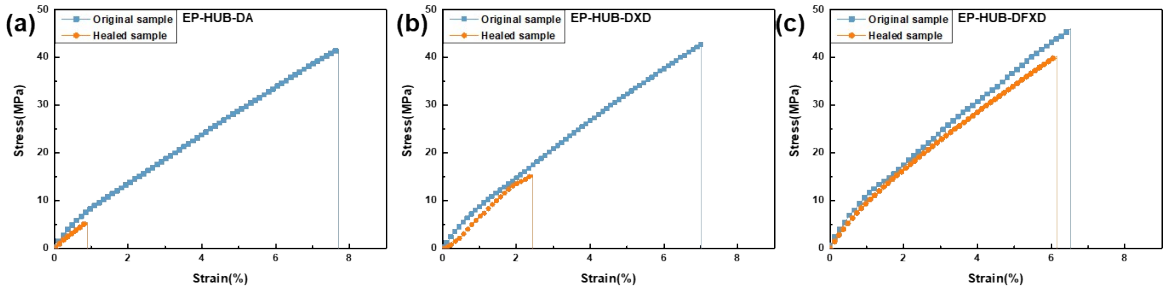

Figure S11. Stress–strain curves of epoxy containing hindered urea bonds with different molecular structures before and after cut-healing.

Table S3. Comparison of the healability of EP-HUB-DFXD with recently reported healable epoxy resins.

References	Healability for mechanical damage	Healability for electrical damage
[1]	Fracture damage; η(tensile strength): 78% η(elongation at the break): 88.3%	Not available
[2]	Fracture damage; η(tensile strength): 59% η(elongation at the break): 58%	Not available
[3]	Not available	Electrical trees damage The healing time is more than 24 h
[4]	Not available	Electrical trees damage The healing time is 16 h
[5]	Not available	Electrical trees damage The healing time is more than 48 h
[6]	Scratch damage	Electrical trees damage The healing time is 30 min
[7]	Scratch damage	Electrical trees damage The healing time is 2 h
[8]	Scratch damage	Electrical flashover damage The healing time is 1 h
This work	**Fracture damage;** **η(tensile strength): 91%** **η(elongation at the break): 89%**	**Electrical trees damage** **The healing time is 30 min**

Table S4. Chemical resistance of EP-HUB-DFXD

Type of solvents	H_2SO_4 (0.1 mol/L)	CH_3COOH (5%)	NaOH (0.1 mol/L)	$NH_4{\cdot}OH$ (10%)	EA	DBA
Mass loss percentage	1.8%	2.0%	2.1%	1.9%	2.9%	1.6%

Table S5. Comparison of the degradability of EP-HUB-DFXD with recently reported degradable epoxy materials.

References	**Dynamic Bond Species**	**Degradation conditions**	**Degree of degradation**	**Components recovery**

[9]	Dynamic ester	Ethanol solvent/140 ℃	Fully degraded	Degraded resins
[10]	Dynamic disulfide	1-octanethiol/ 100 ℃	Partially degraded	Degraded resins
[11]	Dynamic imine bond	0.1 mol/L HCl	Fully degraded	Fiber and degraded resins
[12]	Dynamic ester bond	0.1 mol/L NaOH/ 50 ℃	Fully degraded	Degraded resins
[13]	Dynamic disulfide	5 wt% NaOH	Fully degraded	Degraded resins
[14]	Boronic ester	THF/H_2O_2/HCl	Partially degraded	Degraded resins
This work	**Dynamic urea bond**	**Amine solvent /180 ℃**	**Fully degraded**	**Fiber, fillers, degraded resins and device**

References

[1] Chen BF, Liu XH, Liu JM, et al. Intrinsically self-healing, reprocessable and recyclable epoxy thermosets based on dynamic reversible urea bonds. *Rect. Funct. Polym.* 2022;172:105184.

[2] Liu XH, Song X, Chen BF, et al. Self-healing and shape-memory epoxy thermosets based on dynamic diselenide bonds. *Rect. Funct. Polym.* 2022;170:105121.

[3] Xie JY, Gao L, Hu J, Li Q, He JL. Self-healing of electrical damage in thermoset polymers via anionic polymerization. *J. Mater. Chem. C* 2020;8(18):6025-6033.

[4] Gao L, Yang Y, Xie JY, et al. Autonomous self-healing of electrical degradation in dielectric polymers using in situ electroluminescence. *Matter* 2020;2(2):451-463.

[5] Xie JY, Yang MC, Liang JJ, et al. Self-healing of internal damage in mechanically robust polymers utilizing a reversibly convertible molecular network. *J. Mater. Chem. A* 2021;9: 15975.

[6] Sima WX, Liang C, Sun PT, et al. Novel smart insulating materials achieving targeting self-Healing of electrical trees: high performance, low cost, and eco-friendliness. *ACS Appl. Mater. Interfaces* 2021;13(28):33485-33495.

[7] Sun PT, Zhao MK, Sima WX, et al. Microwave-magnetic field dual-response raspberry-like microspheres for targeted and repeated self-healing from electrical damage of insulating composites. *J. Mater. Chem. C* 2022;10(28):10262-10270.

[8] Zhang YC, Li WD, Zhao X, et al. Epoxy-based high-k composite vitrimer: With low dielectric loss, high breakdown strength and surface electrical damage repairability. *Chem. Eng. J.* 2023;473:145199.

[9] Yang XX, Guo LZ, Xu X, et al. A fully bio-based epoxy vitrimer: Self-healing, triple-shape memory and reprocessing triggered by dynamic covalent bond exchange. *Mater. Des.* 2020;186:108248.

[10] Memon H, Wie Y. Welding and reprocessing of disulfide-containing thermoset epoxy resin exhibiting behavior reminiscent of a thermoplastic. *J. Appl. Polym. Sci.* 2020;137(47):e49541.

[11] Liu YY, He J, Li YD, et al. Biobased epoxy vitrimer from epoxidized soybean oil for reprocessable and recyclable carbon fiber reinforced composite. *Compos. Commun.* 2020;22:100445.

[12] Zhou SC, Huang KF, Xu XW, et al. Rigid-and-flexible, degradable, fully biobased thermosets from lignin and soybean oil: Synthesis and properties. *ACS Sustainable Chem. Eng.* 2023;11:3466-3473.

[13] Ma ZY, Wang Y, Zhu J, et al. Bio-based epoxy vitrimers: Reprocessibility, controllable shape memory, and degradability. *J. Polym. Sci., Part A: Polym. Chem.* 2017;55:1790-1799.

[14] Zeng YN, Li JW, Liu SX, et al. Rosin-based epoxy vitrimers with dynamic boronic ester bonds. *Polymers*, *2021*;13:3386.